Contribution from the Guelph-Waterloo Centre for Graduate Work in Chemistry, Guelph Campus, Department of Chemistry and Biochemistry, University of Guelph, Guelph, Ontario, Canada N1G 2W1, and Waterloo Campus, Department of Chemistry, University of Waterloo, Waterloo, Ontario, Canada N2L 3G1

Solid-State ^{31}P NMR Investigations of Phosphido-Bridged Complexes: Chemical Shift/Bond Angle Correlations

A. J. Carty,* C. A. Fyfe,*,† M. Lettinga, S. Johnson, and L. H. Randall

Received November 29, 1988

Solid-state CP/MAS ^{31}P NMR spectra were measured for a series of phosphido-bridged diiron complexes $Fe_2(CO)_6(\mu\text{-}X)(\mu\text{-}PPh_2)$, where X is a three-electron-donor hydrocarbyl ligand, and for the isostructural series $M_2(CO)_6(\mu_2\text{-}\eta^2\text{-}C{\equiv}CR)(\mu\text{-}PPh_2)$ (M = Fe, Ru, Os; R = Bu^t, Pr^i, Ph). The isotropic solid-state shifts correlate rather well with the corresponding shifts in solution, the largest difference being 8.9 ppm, indicating that there are no phase-dependent structural features. Analysis of the principal elements of the shielding tensor by the spinning-sideband method showed a good correlation between the individual tensor components σ_{11}, σ_{22}, and σ_{33} or composite measures of these and the M-P-M bond angle. The increase of isotropic shift with M-P-M appears to reflect a large change in the σ_{33} tensor component, and the correlations observed suggest that all of the compounds studied have common shift tensor orientations with respect to the molecular frame. Experimental techniques for optimizing the acquisition of solid-state ^{31}P spectra are discussed.

Introduction

Especially since the advent of pulse-FT techniques and multinuclear capabilities, high-resolution solution NMR spectroscopy has developed into the most widely used technique for the determination of unknown chemical structures. In these studies, a key feature of the spectra is the diagnostic manner in which the chemical shifts of nuclei reflect their local magnetic environments in terms of chemical functionalities. In the case of organometallic complexes, ^{31}P NMR spectroscopy has been a particularly useful probe of molecular structure, often distinguishing between structurally closely related compounds or isomers.[1,2]

In an attempt to obtain more quantitative information regarding the local chemical environment, there have been numerous attempts to correlate solution NMR chemical shifts with structural parameters such as bond lengths, bond angles, charge densities, etc.[3] The basic assumptions behind this approach are that the chemical shielding of a nucleus reflects the local magnetic environment and that one of the above parameters may be the major contributor determining this local environment (in general, contributions will diminish with distance from the nucleus in question). In the case of transition-metal complexes, such correlations with local geometric factors have been found for the ^{31}P solution NMR chemical shifts of attached phosphine ligands.[2] In the case of phosphido-bridge ligands, the subject of the present work, a reasonable correlation between P-M-P bond angles and the ^{31}P solution shifts of the phosphido bridge has been reported for a series of binuclear group VIII complexes.[4] In addition, solution ^{31}P NMR chemical shift data have played a significant role as a structural probe for a wide variety of phosphido-bridged complexes. Particularly useful have been the empirical observations of high-field shifts for "open" phosphido bridges, i.e. $\mu\text{-}PR_2$ groups bridging nonbonding metal atoms with large M-P-M bond angles, and low-field shifts for $\mu\text{-}PR_2$ ligands bridging strongly interacting metals.[1a]

One possible difficulty with such correlations, which is quite general, is that the spectroscopic parameters are obtained from solution studies whereas the structural data are derived from single-crystal X-ray diffraction experiments. This problem may be circumvented by using high-resolution NMR data obtained from the solid state.[5] Thus, by a combination of high-power proton decoupling[6] to remove dipolar interactions, magic-angle spinning[7] to reduce the chemical shift anisotropy to its average value, and cross-polarization[8] to enhance the S/N, high-resolution NMR spectra may be obtained for a whole range of magnetically dilute nuclei in the solid. An important feature of these spectra is that the observed resonances occur at the isotropic chemical shift values. That is, they have exactly the same meaning as those observed in solution. Thus, chemical shift/structural correlations such as those described above may be attempted by using two data sets obtained from exactly the same phase. In addition, since the shielding of the nucleus is a three-dimensional quantity whose average value is used in the form of the isotropic chemical shift, more detailed information may be obtained from solid-state studies where the complete three-dimensional nature of the shielding may be determined and included in such correlations.

The purpose of the present investigation was to explore this relationship in detail for a carefully chosen series of complexes containing phosphido-bridge ligands whose range of M-P-M bond angles are known from single-crystal diffraction studies[4a] and to compare these values with data obtained from solid-state NMR studies.

Experimental Section

^{31}P CP/MAS NMR spectra were obtained at 36.432 and 81.020 MHz by using Bruker CXP-100 (90 MHz) and CXP-200 spectrometers, respectively, with home-built probes. A CP/MAS probe supplied by Chemagnetics, Fort Collins, CO, was also used at the higher frequency. The "magic angle" of 54°44′ was set experimentally by optimizing the sideband pattern of the ^{79}Br resonance obtained from a small amount of KBr added to the spinner as described by Frye and Maciel.[9] Compounds were prepared as previously described.[4a,10]

Results and Discussion

Choice of Materials. As will be seen below, the isotropic

* To whom correspondence should be addressed: A.J.C., University of Waterloo; C.A.F., University of Guelph.
† Present Address: Department of Chemistry, University of British Columbia, Vancouver, British Columbia, Canada V6T 1Y6.

(1) See, for example: (a) Carty, A. J.; MacLaughlin, S. A.; Nucciarone, D. In *Phosphorus-31 NMR Spectroscopy in Stereochemical Analysis: Organic Compounds and Metal Complexes*; Verkade, J. G., Quin, L. D., Eds.; VCH Publishers: New York, 1987; Chapter 16, and references cited therein. (b) Regragui, R.; Dixneuf, P. H.; Taylor, N. J.; Carty, A. J. *Organometallics* **1986**, *5*, 1.
(2) Pregosin, P. S.; Kunz, R. W. In *^{31}P and ^{13}C NMR of Transition Metal Complexes*; Diehl, P., Fluck, E., Kosfeld, R., Eds.; NMR Basic Principles and Progress 16, Springer-Verlag: Berlin, 1979, and references cited therein.
(3) See for example: (a) Fluck, E.; Heckmann, G. In *Phosphorus-31 NMR Spectroscopy in Stereochemical Analysis: Organic Compounds and Metal Complexes*; Verkade, J. G., Quin, L. D., Eds.; VCH Publishers: New York, 1987, Chapter 2 and references cited therein. (b) Gorenstein, D. G. In *Phosphorus-31 NMR Principles and Applications*; Gorenstein, D. G., Ed.; Academic Press: New York, 1984, Chapter 1 and references cited therein. (c) Meek, D. W.; Mazanec, T. J. *Acc. Chem. Res.* **1981**, *14*, 266 and references cited therein.
(4) (a) Mott, G. N.; Carty, A. J. *Inorg. Chem.* **1983**, *22*, 2726 and references cited therein. (b) Carty, A. J. *Adv. Chem. Ser.* **1982**, *192*, 163.
(5) Fyfe, C. A. *Solid State NMR for Chemists*; C. F. C. Press: Guelph, Ontario, Canada, 1983.
(6) Schaefer, J.; Stejskal, E. O. *J. Chem. Phys.* **1976**, *98*, 1031.
(7) Andrew, E. R. *Prog. Nucl. Magn. Reson. Spectrosc.* **1971**, *8*, 1.
(8) Pines, A.; Gibby, M. G.; Waugh, J. S. *J. Chem. Phys.* **1972**, *56*, 1776; **1973**, *59*, 569.
(9) Frye, J. S.; Maciel, G. E. *J. Magn. Reson.* **1982**, *48*, 125.
(10) Cherkas, A. A.; Randall, L. H.; MacLaughlin, S. A.; Mott, G. N.; Taylor, N. J.; Carty, A. J. *Organometallics* **1988**, *7*, 969.

0020-1669/89/1328-4120$01.50/0

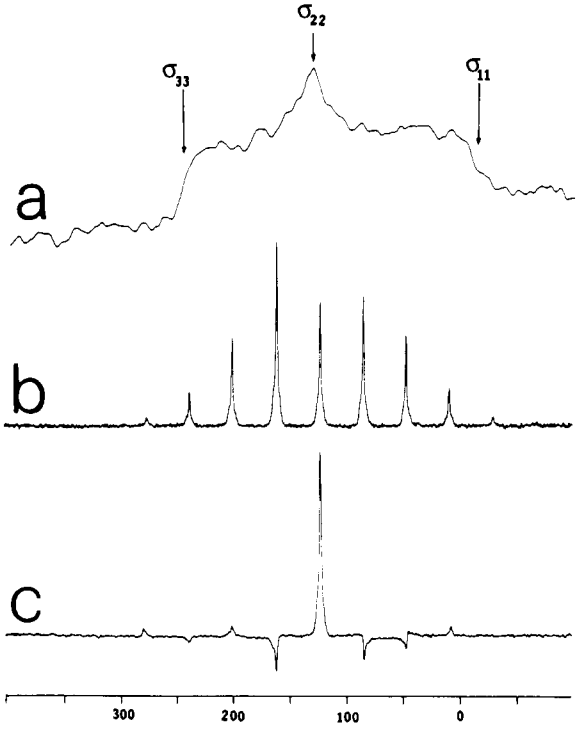

Figure 1. ^{31}P solid-state NMR spectra of $Ru_2(CO)_6(\mu_2\text{-}\eta^2\text{-}C{\equiv}CBu^t)(\mu\text{-}PPh_2)$ obtained at 81.02 MHZ with proton dipolar decoupling: (a) stationary sample with the principal elements of the shielding tensor indicated by the vertical arrows (NS = 4150; recycle time = 30 s); (b) sample spinning at the magic angle with $^1H \rightarrow {}^{31}P$ cross-polarization (rotor frequency = 3058 kHz; NS = 438; contact time = 1 ms; recycle time = 5 s); (c) sample as in part b but with the TOSS sequence used to remove the spinning sidebands.

chemical shift and even the principal elements of the shielding tensor itself give only partial descriptions of the complete magnetic environment of a nucleus. In order to best develop quantitative correlations with structural parameters, it is very important that the compounds studied have a common electronic structure with no variation in the number and nature of the atoms in the immediate vicinity of the nucleus of interest that could alter the nature of the bonding.

In the present work, a series of compounds was examined based on the diphenylphosphido-bridged diiron hexacarbonyl moiety, $Fe_2(CO)_6(\mu\text{-}X)(\mu\text{-}PPh_2)$ (**1**) shown in Chart I. The individual compounds investigated, **2–11**, are also shown in Chart I. As the group X is changed in **1**, the Fe–P–Fe angle is found to vary from 69.8° (X = Cl) to 75.6° (X = $-CH_2C(Ph)NMe$). Although the change is relatively small, the quality of the diffraction data ensures that the individual values are accurate to ±0.1°. We also include solid-state ^{31}P NMR data for the isostructural series of compounds $M_2(CO)_6(\mu_2\text{-}\eta^2\text{-}C{\equiv}CR)(\mu\text{-}PPh_2)$, where M = Fe, Ru, and Os and R = *tert*-butyl (Bu^t), isopropyl (Pr^i), and phenyl (Ph) (complexes **12–19**).

NMR Experiments. As indicated in the Introduction, the chemical shielding of a nucleus is a three-dimensional quantity. Thus, a dipolar-decoupled, cross-polarization spectrum of a resonance in a stationary powdered sample will show a chemical shift anisotropy pattern due to the random orientations of the crystallites (and hence the nuclei therein) to the magnetic field. Formally, the three-dimensional shielding is described by the shift tensor σ, which is a 3 × 3 matrix. This matrix may be transformed into diagonal form by a suitable choice of coordinate system. The diagonal elements σ_{11}, σ_{22}, and σ_{33} are called the principal elements and indicate the characteristic shielding of the nucleus in three orthogonal directions. In a powder pattern, these correspond to the singularities in the spectrum as indicated by the vertical arrows in Figure 1a for the ^{31}P resonance of $Ru_2(CO)_6(\mu_2\text{-}\eta^2\text{-}C{\equiv}CBu^t)(\mu\text{-}PPh_2)$.

Spinning the sample at the magic angle produces the isotropic chemical shift $\sigma_{iso} = {}^1/_3(\sigma_{11} + \sigma_{22} + \sigma_{33})$, the same value as obtained by the isotropic motion of the molecule in solution. If the mechanical spinning frequency is less than the frequency width of the anisotropy pattern, the isotropic peak will be flanked on either side by a series of spinning sidebands whose intensities approximate the profile of the anisotropy pattern (Figures 1b and 2a). If the shift anisotropy is very large, as is often the case for the ^{31}P resonances of phosphorus ligands, including those investigated in the present work, the isotropic peak will be reduced in intensity, often having an intensity less than that of some of the sidebands, and may be difficult to identify. Various methods of sideband suppression exist, and we have explored several in the present work. One obvious solution is to spin at rates proportional to the size of the CSA. At 4.9 T, this means spinning at rates up to 9 kHz to effectively eliminate the sidebands on compounds with even moderate ^{31}P CSA's. Small first-order sidebands still occur in compounds with large anisotropies, but the isotropic peak can still be readily identified (Figure 3b). One drawback to this method is that the spinners used for such high-speed spinning are smaller and the sample volume is reduced, resulting in a loss of S/N. Another possible method is variable-speed spinning accomplished by changing the air pressure to the rotor. Since the position of the sidebands varies directly as the spinning speed, a variation of 1 kHz in spinning speed means that the sidebands will not add in a coherent fashion but will form broad featureless humps (Figure 3a). This method has the advantage of simplicity and could be easily automated.

The method of choice, however, was to use the TOSS (total suppression of spinning sidebands) multiple-pulse sequence introduced by Dixon.[11] As illustrated in Figures 1c and 2b, the

Table I. Solid-State and Solution[a] ^{31}P NMR Isotropic Chemical Shifts for $Fe_2(CO)_6(\mu\text{-}X)(\mu\text{-}PPh_2)$

X	complex	σ_{iso}(solid)	σ_{iso}(soln)	σ_{iso}(solid) − σ_{iso}(soln)	Fe–P–Fe bond angle, deg
Cl	**2**	143.4	142	1.4	69.8 (0)
$CHC(NEt_2)Ph$	**3**	161.5	153.9	7.6	70.1 (0)
$C{=}C(PCy_2H)Ph$	**4**	131.9	123	8.9	70.7 (1)
CHC(NHCy)Ph	**5**	158.3	154	4.3	70.5 (0)
C≡CPh	**6**	155.2	148.4	6.8	71.64 (7)
C(NHCy)CH(Ph)	**7**	189.9	183.5	6.4	72.5 (0)
$C(CNMe(CH_2)_2NMe)CPh$	**8**	191.5	190.3	1.2	73.4 (0)
$C\{P(OEt)_3\}C(Ph)$	**9**	199.3	193.0	6.3	74.0 (0)
$C(CNBu^t)CPh$	**10**	192.7	194.2	−1.5	74.1 (0)
$CH_2C(Ph)NMe$	**11**	205.3	198.5	6.8	75.6 (0)

[a] Solution ^{31}P NMR spectral data were measured on solutions in 10-mm tubes and are relative to external H_3PO_4.

Table II. Calculated Chemical Shift Anisotropy Parameters for $Fe_2(CO)_6(\mu\text{-}X)(\mu\text{-}PPh_2)$[a]

X	complex	σ_{11}	σ_{22}	σ_{33}	μ[b]	$\Delta\sigma$[c]	η,[d] %
Cl	**2**	58	135	237	179	140	86
$CHC(NEt_2)Ph$	**3**	74	125	286	212	186	48
$C{=}C(PCy_2H)Ph$	**4**	22	130	243	221	167	98
CHC(NHCy)Ph	**5**	71	122	282	211	185	48
C≡CPh	**6**	32	154	279	247	186	99
C(NHCy)CH(Ph)	**7**	10	182	377	367	281	94
$C(CNMe(CH_2)_2NMe)CPh$	**8**	11	155	408	397	325	73
$C\{P(OEt)_3\}C(Ph)$	**9**	10	160	429	419	344	72
$C(CNBu^t)CPh$	**10**	6	160	412	406	329	76
$CH_2C(Ph)NMe$	**11**	5	151	460	455	382	64

[a] From graphical analysis of spinning sideband intensities.[13] Estimated errors for σ_{11}, σ_{22}, and σ_{33} are ±5%. These errors were estimated from the areas of convergence at several spinning rates. The convention $\sigma_{33} > \sigma_{22} > \sigma_{11}$ has been used. [b] $\mu = \sigma_{33} - \sigma_{11}$. [c] $\Delta\sigma = \sigma_{33} - {}^1/_2(\sigma_{22} + \sigma_{11})$. [d] $\eta = 1 - |\rho|$ where $\rho = (\sigma_{33} - 2\sigma_{22} + \sigma_{11})/(\sigma_{33} - \sigma_{11})$.

(11) (a) Dixon, W. T.; Schaeffer, J.; Sefcik, M. D.; Stejskal, E. O.; McKay, R. A. *J. Magn. Reson.* **1982**, *49*, 341. (b) Dixon, W. T. *J. Chem. Phys.* **1982**, *77*, 1800.

Table III. Solid-State and Solution ^{31}P NMR Isotropic Chemical Shifts of $M_2(CO)_6(\mu_2\text{-}\eta^2\text{-}C{\equiv}CR)(\mu\text{-}PPh_2)$ (M = Fe, Ru, Os; R = Ph, Bu^t, Pr^i)[a]

		complex	σ_{iso}(solid)	σ_{iso}(soln)	σ_{iso}(solid) − σ_{iso}(soln)	Fe–P–Fe bond angle, deg
M = Fe	R = Ph	**6**	155.2	148.3	6.9	71.64 (7)
	R = Pr^i	**12A**	154.3	149.7	4.6	71.81 (4)
	R = Pr^i	**12B**	150.5	149.7	0.8	71.39 (4)
	R = Bu^t	**13**	149.8	148.4	1.4	71.7 (0)
M = Ru	R = Ph	**14**	129.5	130.5	−1	
	R = Pr^i	**15**	135	126.1	8.9	
	R = Bu^t	**16**	123.2	125.2	−2	72.03 (1)
M = Os	R = Ph	**17**	51.2	47.3	3.9	
	R = Pr^2	**18**	57.5	48	9.5	
	R = Bu^t	**19**	50.2	45.2	5	72.61 (7)

[a] Solution ^{31}P NMR spectral data were measured on solutions in 10-mm tubes and are relative to external H_3PO_4.

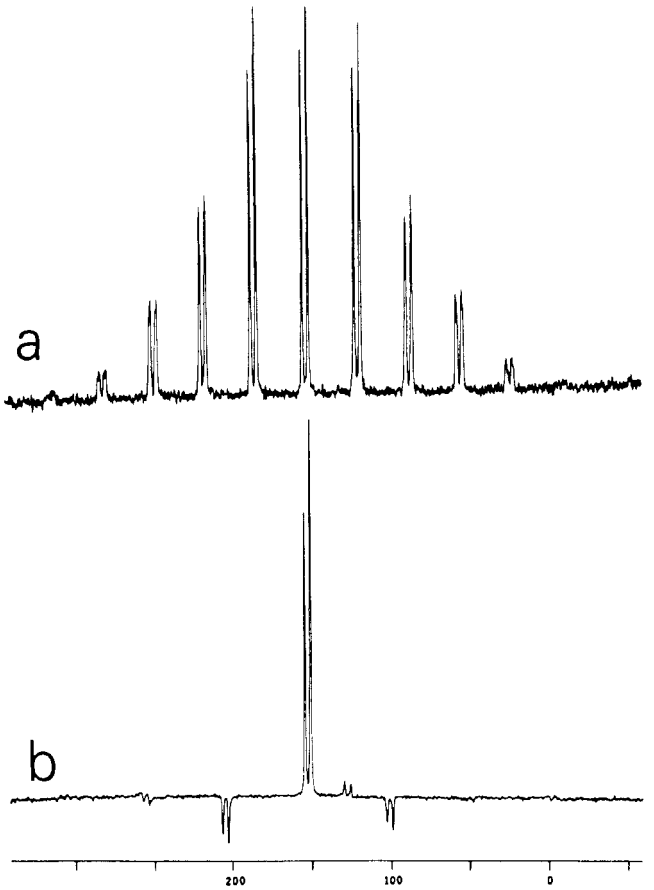

Figure 2. ^{31}P solid-state NMR spectra of $Fe_2(CO)_6(\mu_2\text{-}\eta^2\text{-}C{\equiv}CPr^i)(\mu\text{-}PPh_2)$ obtained at 81.02 MHz by using proton dipolar decoupling and $^1H \rightarrow {}^{31}P$ cross-polarization: (a) sample spinning at the magic angle (rotor frequency = 4.16 kHz; contact time = 1 ms; recycle time = 5 s; NS = 960); (b) sample as in part a but with the TOSS sequence used (NS = 3000).

isotropic peak or peaks are easily identified, although the sideband intensities are lost and not added to a large degree to the isotropic peak. Values of σ_{iso} obtained in this way for all of the compounds studied are tabulated in Tables I and III.

The principal elements of the shielding tensor may be obtained directly from a powder pattern as illustrated in Figure 1a. However, in many cases, there are difficulties in obtaining spectra of good enough S/N to accurately determine the singularities. A second problem with this method is that where there is more than one resonance present, e.g. Figure 2a, the overlap of the powder patterns will preclude analysis of the individual sets of principal elements. A better approach to this problem, which circumvents the difficulties of both S/N and overlap of anisotropy patterns, is to deduce the principal shielding elements from the pattern of spinning sidebands where both sensitivity and resolution

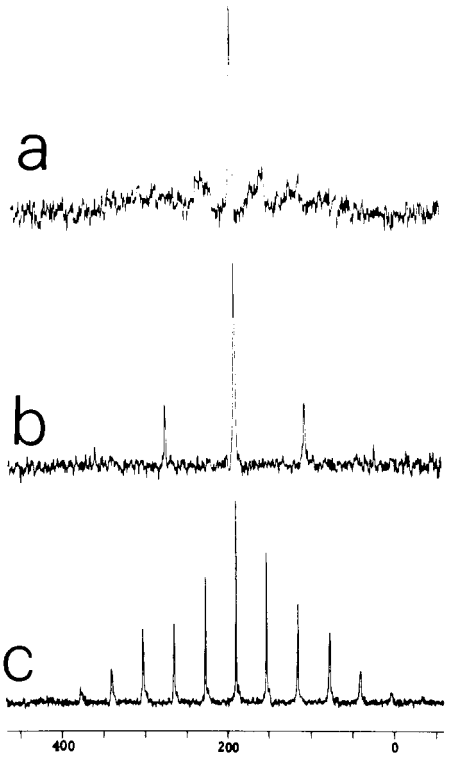

Figure 3. ^{31}P solid-state NMR spectra of $Fe_2(CO)_6[\mu_2\text{-}\eta^2\text{-}C(NHCy)C(H)Ph](\mu\text{-}PPh_2)$ obtained at 81.02 MHz by using proton dipolar decoupling and $^1H \rightarrow {}^{31}P$ cross-polarization (contact time = 1 ms; recycle delay = 1 s): (a) variable rotor frequency, NS = 1200; (b) rotor frequency = 8.80 kHz, NS = 3480; (c) rotor frequency = 3.04 kHz, NS = 3600.

Table IV. Calculated Chemical Shift Anisotropy Parameters for $M_2(CO)_6(\mu\text{-}PPh_2)(\mu_2\text{-}\eta^2\text{-}C{\equiv}CR)$[a]

		complex	σ_{11}	σ_{22}	σ_{33}	μ[b]	$\Delta\sigma$[c]	η,[d] %
M = Fe	R = Ph	**6**	32	154	279	247	186	98
	R = Pr^i	**12A**	34	146	283	249	193	90
	R = Pr^i	**12B**	25	147	278	253	192	96
	R = Bu^t	**13**	28	152	268	240	178	97
M = Ru	R = Ph	**14**	1.0	139	249	248	179	89
	R = Pr^i	**15**	−8	143	269	277	202	91
	R = Bu^t	**16**	−10	136	243	253	176	84
M = Os	R = Ph	**17**	−74	104	128	202	113	23
	R = Pr^i	**18**	−73	110	137	210	118	25
	R = Bu^t	**19**	−74	96	129	206	118	34

[a] From graphical analysis of spinning sideband intensities.[13] Estimated errors in σ_{11}, σ_{22}, and σ_{33} are ±5%. The convention $\sigma_{33} > \sigma_{22} > \sigma_{11}$ has been used. [b] $\mu = \sigma_{33} - \sigma_{11}$. [c] $\Delta\sigma = \sigma_{33} - {}^1/_2(\sigma_{22} + \sigma_{11})$. [d] $\eta = 1 - |\rho|$ where $\rho = (\sigma_{33} - 2\sigma_{22} + \sigma_{11})/(\sigma_{33} - \sigma_{11})$.

are maintained. Two general methods are available for the analysis of the sideband pattern, the moment method of Maricq and Waugh[12] and the graphical analysis of Herzfeld and Berger.[13]

Chart I

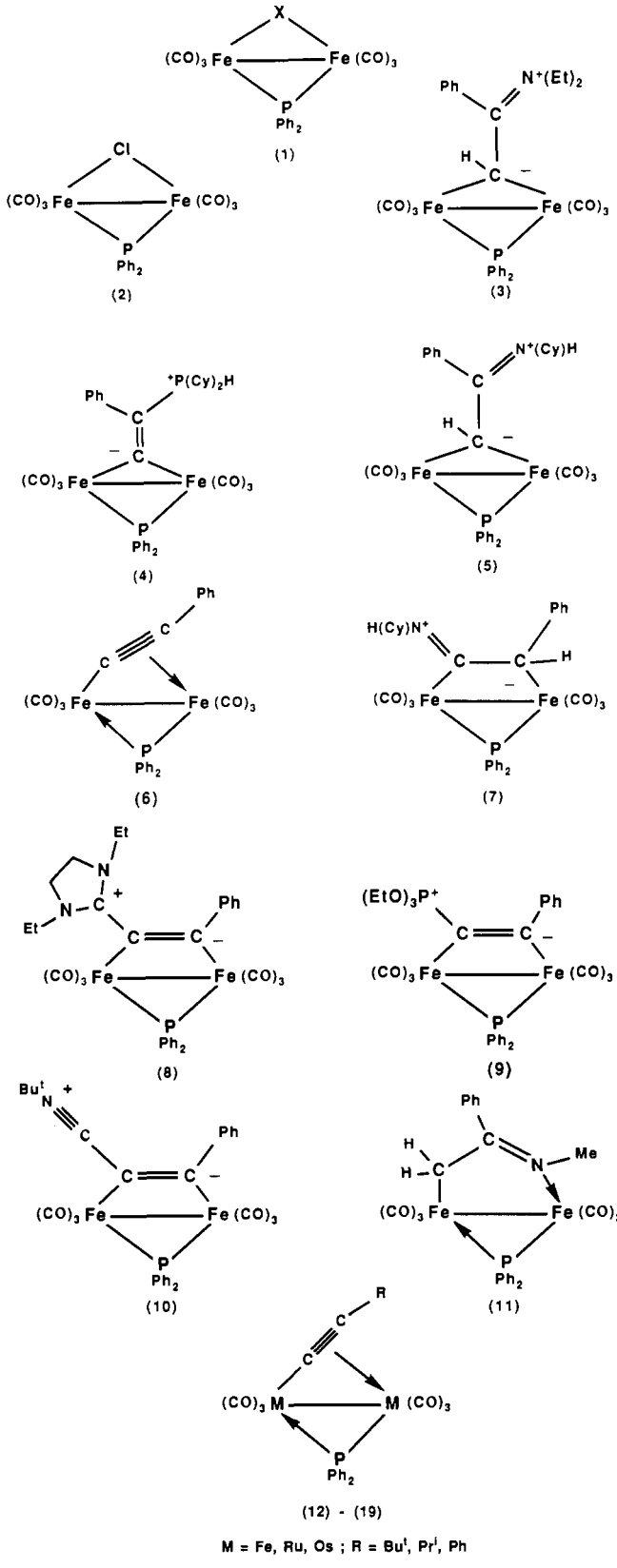

Values of the principal elements of the shielding tensors obtained by the latter technique for all of the compounds studied are given in Tables II and IV.

Chemical Shift Correlations for Complexes 2–11. In the search for correlations between solution and solid-state NMR data and structural parameters, several important factors must be recog-

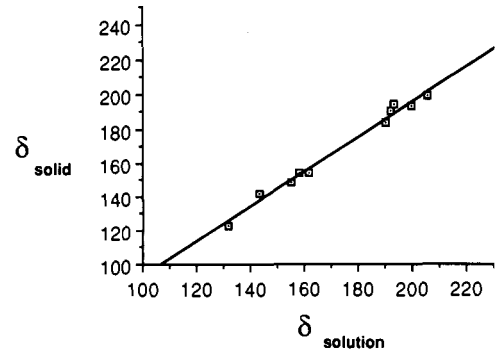

Figure 4. Plot of the isotropic chemical shifts of $Fe_2(CO)_6(\mu\text{-}X)(\mu\text{-}PPh_2)$ in solution vs those in the solid state.

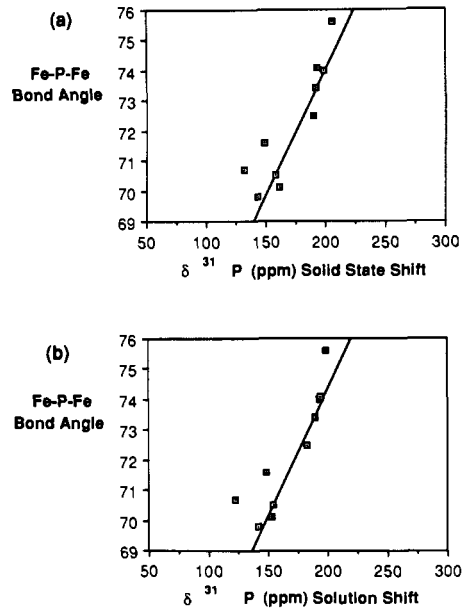

Figure 5. (a) Dependence of the solid-state isotropic chemical shifts of $Fe_2(CO)_6(\mu\text{-}X)(\mu\text{-}PPh_2)$ on the M–P–M bond angles. (b) Dependence of the solution chemical shifts of $Fe_2(CO)_6(\mu\text{-}X)(\mu\text{-}PPh_2)$ on the M–P–M bond angles.

nized. First, both sets of data will reflect a complex set of interactions as the measurements are not being made on isolated molecules; in solution, there will be solvent effects on the shifts, and in the solid-state, molecular packing in the lattice will cause similar (small) variations in local susceptibilities from one lattice structure to another. Second, the solid-state NMR shifts relate directly to the X-ray data. The structure in solution may be different, and deviations in the solution NMR data may arise from this source. Certainly, a large discrepancy between the two sets of isotropic shifts will indicate a change in structure. Third, in both the solution and the solid state, the isotropic chemical shifts are the average of the three principal elements of the shielding tensor. This averaging may well obscure a real correlation within the individual anisotropy parameters. Further, the principal elements determined from powder NMR data yield only the magnitudes and not the directional elements of the shielding. Changes in the orientation of the principal elements will destroy a correlation involving only the magnitudes, and care must be taken to make comparisons only within a series of closely related structures such as those selected in the present work.

With these factors in mind, we discuss the various correlations and deductions that can be made from the data in Tables I and II. Figure 4 shows the isotropic chemical shifts from solution data plotted against those obtained in the solid state. The excellent linear relationship between the two with no large specific deviations, given the environmental contributions to both measurements, indicates that there are no substantial changes in structure between the solid state and the solution for any of the complexes in the series. This correspondence is reflected in Figure 5a,b where both sets of data correlate equally well with the Fe–P–Fe bond angle,

(12) Maricq, M. M.; Waugh, J. S. *J. Chem. Phys.* **1979**, *70*, 3300.
(13) Herzfeld, J.; Berger, A. E. *J. Chem. Phys.* **1980**, *73*, 6021.

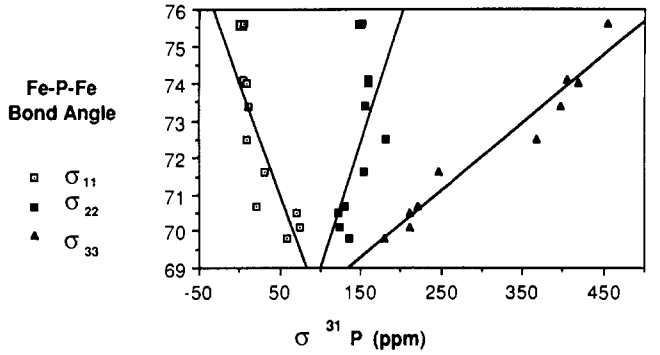

Figure 6. Dependence of the principal elements of the chemical shift tensor of $Fe_2(CO)_6(\mu\text{-}X)(\mu\text{-}PPh_2)$ on M–P–M bond angles.

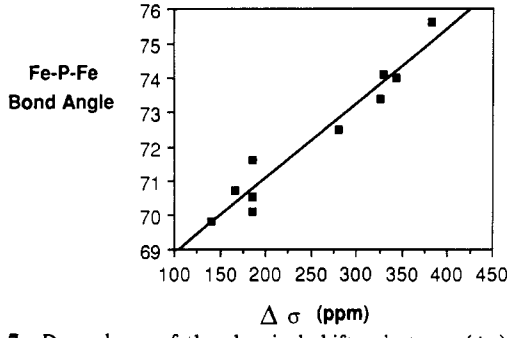

Figure 7. Dependence of the chemical shift anisotropy ($\Delta\sigma$) of $Fe_2(CO)_6(\mu\text{-}X)(\mu\text{-}PPh_2)$ on M–P–M bond angles.

the small displacement between the two lines probably being due to the different referencing of the two sets of spectra. There are significant deviations, most notably involving compounds **4**, **6**, and **11**. The fact that they occur in both correlations indicates that they are due to deficiencies in the correlation attempted and not to differences in structure with the change in state.

Further insight may be obtained from the correlation of the individual tensor components σ_{11}, σ_{22}, and σ_{33} with the Fe–P–Fe angle, as shown in Figure 6. Even with the much larger errors expected for these parameters from the indirect manner in which they are obtained, the correlation is much better than that with the isotropic shift values, indicating that the latter parameters do not adequately reflect the changes manifest in Fe–P–Fe bond angles. σ_{11} shows a small shift to higher field with increasing bond angle, σ_{22} is almost unaffected, and σ_{33} demonstrates the largest dependence on the bond angle, exhibiting a large downfield shift with increasing angle. Most importantly, compounds **4**, **6**, and **11** correlate much better than in the isotropic peak analysis.

In an attempt to incorporate the three-dimensional nature of the shielding into a single parameter, possible correlations with the chemical shift anisotropy ($\Delta\sigma$) and the asymmetry (η),[14] each of which incorporates some elements of the three-dimensional nature of the shielding, were explored.

As can be seen from Table II, there is no obvious correlation between the asymmetry parameter and the bond angle although the nature of the equation means that there could be very large associated errors. On the other hand, the chemical shift anisotropy correlates well as shown in Figure 7. In addition, μ, which relates to the total breadth of the anisotropy pattern and is thus a measure of the deviation from spherical symmetry in two orthogonal directions, also correlates well.

The $M_2(CO)_6(\mu_2\text{-}\eta^2\text{-}C{\equiv}CR)(\mu_2\text{-}PPh_2)$ Series. The ^{31}P chemical shifts of complexes **12**–**19** (Table III) are characteristic of μ-PPh_2 groups bridging across a strong metal–metal bond.[1a] The upfield shifts of ~15 ppm between Fe and Ru and ~80 ppm between Ru and Os are entirely typical and can be used diagnostically for related complexes. The differences between the solid-state isotropic shifts and the solution shifts are quite small and indicate that there are no substantial changes between the two phases. However, neither the isotropic solid-state shifts nor the solution shifts for $M_2(CO)_6(\mu_2\text{-}\eta^2\text{-}C{\equiv}CBu^t)(\mu\text{-}PPh_2)$ relate closely to the M–P–M bond angles as the metal changes. This is of course not unexpected and emphasizes the fact that comparisons can only be made within a series of closely related structures of the *same* transition metal.

In the ^{31}P NMR solid-state spectrum of $Fe_2(CO)_6(\mu_2\text{-}\eta^2\text{-}C{\equiv}CPr^i)(\mu\text{-}PPh_2)$, two isotropic resonances were obtained (Figure 2b). We undertook an X-ray crystallographic study in order to resolve this matter and have found two independent molecules in the asymmetric unit.[15] The slightly different environments for the two molecules in the unit cell result in slightly different Fe–P–Fe bond angles [71.81 (4) and 71.39 (4)°]. Apparently, these two molecules give rise to the two ^{31}P isotropic shifts, and the difference in shifts may be attributed to differences in the Fe–P–Fe bond angles, since no other significant structural differences were observed. The difference in bond angles observed for the two independent molecules (0.4°) corresponds to a difference of isotropic shifts of approximately 3.8 ppm. The solid-state spectrum of this complex (Figure 2) clearly shows the two ^{31}P resonances, a remarkable illustration of the power of solid-state NMR for probing minor structural changes.

Conclusions

Two conclusions that can be drawn from the present work and that establish a sound basis for the correlation of phosphido-bridge angles with ^{31}P chemical shifts are as follows: (i) The equivalence of the solution and solid-state chemical shifts indicates that there are no phase-dependent structural features that are important in this series. (ii) There is a moderately good correlation between the isotropic shifts and the bond angles but much better ones exist between either the individual tensor components or composite measures of these and the bond angles. This indicates that the chemical shielding of the ^{31}P nucleus does quantitatively reflect the changes in geometry around phosphorus but that the isotropic average provides only a rough probe of these changes. Thus, the analysis of individual tensor components from solid-state NMR spectra and their correlation with molecular parameters will be useful in structural studies in these and related systems.

A third conclusion from the present work is that the correlations of Figures 4 and 5 suggest that all of the iron compounds studied have common shift tensor orientations as major differences would destroy any correlations based only on the magnitudes of the shielding parameters. A complete understanding of the relationship between shift parameters and geometric factors necessitates a knowledge of the orientation of the shift tensor with respect to the molecular geometry. This information must be obtained from single-crystal work, and the present correlations provide a justification for performing a limited number of such studies on complexes that can be obtained as crystals of sufficient size.

(14) $\Delta\sigma = \sigma_{33} - {}^1/_2(\sigma_{22} + \sigma_{11})$ and $\eta = 1 - |\rho|$, where $\rho = (\sigma_{33} - 2\sigma_{22} + \sigma_{11})/(\sigma_{33} - \sigma_{11})$.

(15) Cherkas, A. A.; Taylor, N. J.; Lettinga, M. L.; Carty, A. J.; Fyfe, C. A. Unpublished results.